ARCHIVES OF ACOUSTICS
22, 4, 397–410 (1997)

THEORETICAL AND EXPERIMENTAL ANALYSIS OF THE BAND NOISE RADIATED FROM A HARD-WALLED CYLINDRICAL DUCT

A. SNAKOWSKA

Institute of Physics, Pedagogical University
(34-310 Rzeszów, Rejtana 16a, Poland)

H. IDCZAK

Institute of Telecommunication and Acoustics,
Wrocław Technical University,
(50-370 Wrocław, Wybrzeże Wyspiańskiego 27, Poland)

The paper presents, basing on the results obtained for the single tone and multitone excitations, the theory of the white noise propagation in and radiation from a cylindrical duct. The duct is assumed to be semi-infinite and hard walled, the excitation axisymmetrical and with no mean flow.

Solution of the wave equation with adequate boundary condition constitutes a base of the carried out analysis. It allows for propagation of certain number of wave modes, which cut-on frequencies are below the excitation frequency. Anyhow, when more than one mode are present the analysis of the sound field complicates, as it requires the knowledge of modes complex amplitudes.

To make any quantitative comparison between the theory and experiment possible two extra assumptions are incorporated into the theory: on the equipartition of the density of energy between all modes admissible at a given frequency and on their random phase. The second assumption results in the necessity of describing the acoustical field by means of the expected value, the variance and the standard deviation of the pressure, the intensity, the power output etc.

The paper contains the directivity characteristics of the pressure and the intensity and evaluation of the power output for the one third octave (tierce) band white noise.

1. Introduction

The aim of the presented paper is to extend the theory of sound wave propagating in and radiating from a circular duct on a case of narrow-band white noise excitation.

The theory of propagation of acoustic waves in a semi-infinite duct predicts that at a given frequency only some waves can propagate without damping [2, 3, 15]. The quantity which is the most convenient for investigations on this problem is the non-dimensional wavenumber, ka, being a product of the wave number k and the duct radius a, and so combining the wave frequency with the duct size. Apart from the plane wave which

propagates at any ka the occurrence of any higher mode is specified by the so-called cut-on frequency. Propagation of the plane wave or single higher mode, in a duct excited with a single tone signal has been considered by many authors, who applied the so-called time independent form of the velocity potential [11, 25, 26, 6, 8, 9, 13, 14, 22].

In the following we consider a case in which the duct is excited with a narrow-band white noise. That means that the velocity potential has to be written as a sum over all allowed modes and an integral over frequencies.

The theory of sound field inside and outside the duct has been a subject of our interest since long. Especially, we have analysed the far field of a single higher mode by means of the directivity patterns (pressure, intensity, power-gain function) [17]. Next step has been to derive the directivity characteristics for an arbitrary superposition of modes, what has led to a conclusion that directivity strongly depends on complex amplitudes i.e. on the modulae and phases of the excited modes [18].

That means that a set of numbers representing the modulae and phases has to be inserted into mathematical formulae to make any predictions about the radiation characteristics, the power output etc., or comparison with the experimental data possible.

To deal with these drawbacks the model composed of two assumptions [21] is proposed

— the total energy is shared in equal parts between all excited modes,

— phases are independent random variables with the uniform distribution in the range $[0, 2\pi]$.

The first assumption, often called "equal energy per mode" has been successfully applied by many authors [1, 14, 19, 21], the second assumption seems to be well physically justified – if there is no knowledge what exactly the phases are the best solution is to assume them being random [21].

2. Analysis technique and results

2.1. Mathematical background. Solution of the wave equation for the single tone excitation

Mathematical tools applied to obtain a solution of the problem are rather complicated and include the theory of two-valued analytical functions, application of the Green function in the cylindrical coordinates, the solution of the Wiener-Hopf integral equations by means of the factorisation method, the saddle point method etc., so there will be reminded only in short.

Consider the wave equation for the acoustic potential $\Delta\Phi(\mathbf{r}, t) = c^{-2}\partial_{tt}\Phi(\mathbf{r}, t)$, with adequate boundary condition given on the duct surface (Fig. 1) $v_{\mathrm{n}} = -\partial_{\mathrm{n}}\Phi|_{\Sigma} = 0$, and assume an axisymmetrical harmonic excitation of given frequency ω.

First, the solution of the wave equation for a single l mode propagating towards the outlet will be reminded – in cylindrical coordinates ϱ, φ, z, for inside of the duct [26]

$$\Phi_l(\omega, \varrho, z, t) = \left[\frac{J_0(\mu_l \varrho/a)}{J_0(\mu_l)} e^{-i\gamma_l z} + \sum_{n=0}^{N} R_{ln} \frac{J_0(\mu_n \varrho/a)}{J_0(\mu_n)} e^{i\gamma_n z}\right] e^{-i\omega t}, \tag{2.1}$$

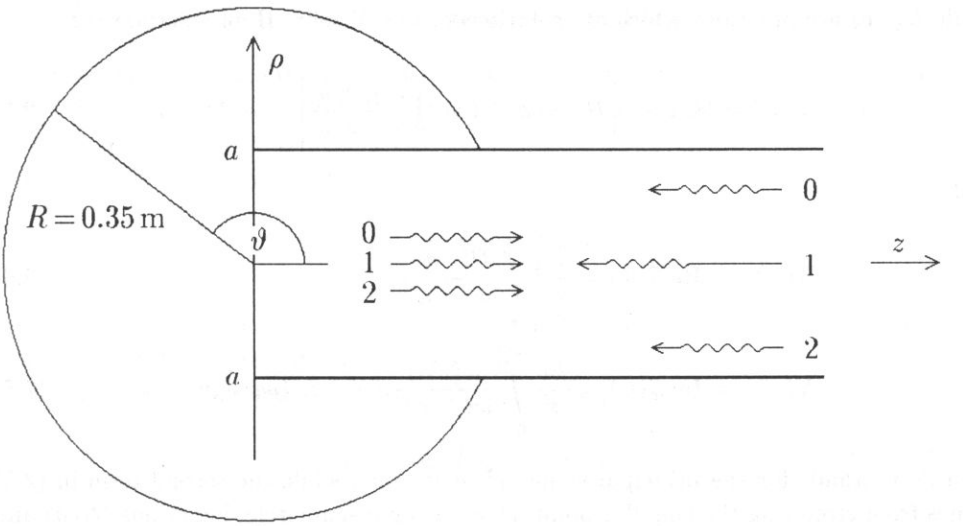

Fig. 1. Geometry of the problem.

and in spherical coordinates R, ϑ, φ, in the far field outside the duct [17]

$$\Phi_l(\omega, R, \vartheta, t) = d_l(\vartheta)\frac{e^{i(kR-\omega t)}}{R}. \tag{2.2}$$

The incident wave, l radial mode, described by the first factor in (2.1), propagates with the radial wave number $\gamma_l = \sqrt{(ka)^2 - \mu_l^2}/a$, where μ_l is the l-th zero of the Bessel function J_1. Terms under the summation sign represent waves appearing due to diffraction at the outlet, where R_{ln} is the reflection/transformation coefficient. The number of admissible modes depends on the dimensionless parameter ka, called also the non-dimensional wavenumber. The index of the highest mode, which propagates without attenuation fulfils the condition $\mu_N < ka < \mu_{N+1}$. For a duct of radius a the cut-on frequencies ω_l are equal to $\omega_l = c_0\mu_l/a$, where c_0 is the sound speed.

In the far field outside the duct the incident lth mode propagates as a spherical wave modified by the directivity function d_l, which in general is a function of R, ϑ. In the following we will concentrate on the infinite distance approximation ($kR \to \infty$), when the directivity function, derived by means of the saddle point method, is a function of only the angle ϑ [17] (Fig. 1)

$$d_l(\vartheta) = \frac{1}{2}ka\sin\vartheta J_1(ka\sin\vartheta)F_l(ka\cos\vartheta). \tag{2.3}$$

The method itself, successfully applied to many acoustical problems, is described in [12]. Mathematical considerations leading to (2.3), reported in [17, 22], especially deriving the $F_l(w)$ function, which in fact is the Fourier transform of the discontinuity of potential $\Phi(\varrho, z)|_{\varrho\to a+} - \Phi(\varrho, z)|_{\varrho\to a-}$ at the duct wall, are rather complicated.

Assuming a unit amplitude of the incident wave we obtain [17]

$$F_l(w) = \frac{L_+(\gamma_l)}{i(w+\gamma_l)L_-(w)}, \tag{2.4}$$

while $L_{\pm}(w)$ are functions which are solutions of the Wiener - Hopf equation [12]

$$L_{\pm}(w) = (k \pm w)\left[H_1^{(1)}(va)J_1(va)\prod_{i=1}^{N}\frac{\gamma_i \pm w}{\gamma_i \mp w}\right]^{1/2} e^{\pm\frac{1}{2}S(w)}, \tag{2.5}$$

and

$$\mathrm{X}(w) = \mathrm{Re}\,S(w) = \frac{1}{\pi}\mathrm{P}\int_{-k}^{k}\frac{\Omega(v'a)}{w'-w}\,dw', \tag{2.6}$$

$$\mathrm{Y}(w) = \mathrm{Im}\,S(w) = \frac{2w}{\pi}\int_{0}^{i\infty}\frac{\omega(v'a)}{w^2-w'^2}dw' + i\omega(va)\mathrm{sign}w. \tag{2.7}$$

P in (2.6) stands for the principal value, $w^2 + v^2 = k^2$, while the second term in (2.5) comes from circuiting the singular point $w' = \pm w$ on a semicircle. Functions $\Omega(va)$ and $\omega(va)$ are equal to

$$\Omega(va) = \arg H_1^{(1)}(va) + \pi/2\,, \tag{2.8}$$

$$\omega(va) = \Omega(va) - \Omega(\mu_n), \qquad \mu_n < va < \mu_{n+1}\,. \tag{2.9}$$

The $L_+(w)$ function for $w = \gamma_n$ exists only as a limited value for $w \to \gamma_n$ and is equal to

$$L_+(\gamma_l) = \begin{cases} 2k\left(\dfrac{-i}{\pi}\displaystyle\prod_{i=1}^{N}\frac{\gamma_i + k}{\gamma_i - k}\right)^{1/2} e^{\frac{1}{2}S(k)}, & l = 0, \\ \dfrac{2(k+\gamma_l)\gamma_l a}{\mu_l}\left(\dfrac{-i}{\pi}\displaystyle\prod_{\substack{l=1\\ i\neq l}}^{N}\frac{\gamma_i + \gamma_l}{\gamma_i - \gamma_l}\right)^{1/2} e^{\frac{1}{2}S(\gamma_l)}, & l \neq 0, \end{cases} \tag{2.10}$$

where $\gamma_0 = k$.

Because of mathematical complexity of the problem a set of numerical programs has been derived, which enables us to present the reflection coefficients, the directivity functions etc. graphically and to carry out a thorough analysis of the sound field of interest.

Previously we assumed a unit amplitude incident wave. As was mentioned before, the theory foresees and the experiments, in which the power spectra density [1] and the directivity characteristics [21] were measured, confirm excitation of all admissible modes. If N indicates the highest Bessel mode and A_l is a complex amplitude, we can write the potential in the form

$$\Phi = \sum_{l=0}^{N} A_l \Phi_l\,. \tag{2.11}$$

2.2. *The white noise excitation*

Basing on the results obtained for excitation with a fixed frequency [21] we will extend the formulae for the potential, the mean pressure and the intensity on the case of continues spectrum of frequencies.

For the white noise we obtain

$$\phi(\bar{r},t) = \int\limits_{\omega\in B} \phi(\omega,\bar{r},t)\,\varrho(\omega)\,d\omega\,, \tag{2.12}$$

where $\varrho(\omega)$ is the spectral density of energy and B is the band width. In the following we assume constant spectral density $\varrho(\omega) = 1$.

Thus, the acoustic pressure, $p = \varrho_0 \partial_t \Phi$, can be expressed as

$$p(\bar{r},t) = \int\limits_{\omega\in B} p(\omega,\bar{r},t)\,d\omega\,, \tag{2.13}$$

where

$$p(\omega,R,\vartheta,t) = \varrho_0\omega \sum_{l=0}^{N} A_l(\omega) d_l(\omega,R,\vartheta)\frac{e^{i(kR-\omega t-\pi/2)}}{R} = \sum_{l=0}^{N} P_l(\omega,R,\vartheta)e^{i(-\omega t+\theta_l)}\,, \tag{2.14}$$

is an extension of the formula for a single tone excitation [21].

The pressure real amplitude P_l and phase θ_l were expressed by the modulus and phase of the complex amplitude $A_l = |A_l|e^{i\phi_l}$:

$$P_l(\omega,R,\vartheta) = \frac{\varrho_0}{R}\omega|A_l(\omega)|d_l(\omega,R,\vartheta), \qquad \theta_l = kR + \phi_l - \pi/2\,. \tag{2.15}$$

According to the first assumption, for each frequency ω the modulae of amplitudes are related as follows

$$\left|\frac{A_m(\omega)}{A_l(\omega)}\right| = \sqrt{\frac{\gamma_l(\omega)}{\gamma_m(\omega)}}\,. \tag{2.16}$$

According to the second assumption, for each frequency, phases are stochastically independent random variables.

Below presented formulae are valid in an infinite distance approximation ($kR \to \infty$). To indicate this the variable R is omitted and we write, for example, $I(\vartheta)$ instead of $I(R,\vartheta)$

$$I(\vartheta) = \frac{1}{2\varrho_0 c}\int\limits_{\omega\in B}\left[\sum_{l=0}^{N(\omega)} P_l^2 + 2\sum_{\substack{l,m\\ l<m}}^{N(\omega)} P_l\,P_m\cos(\phi_l-\phi_m)\right]d\omega\,. \tag{2.17}$$

Note that the intensity depends on the phase differences between modes of the same frequency ω.

Note that the same results can be achieved exchanging operation of summation over some discrete frequencies [20] for integration over a certain frequency band.

For constant power spectral density, choosing the amplitude of the principal mode (plane wave, $m = 0$) at the mid-frequency ω_0 as the reference amplitude we obtain

$$|A_0(\omega)|^2 = \frac{N(\omega_0)+1}{N(\omega)+1}\left(\frac{\omega_0}{\omega}\right)^2 |A_0(\omega_0)|^2. \tag{2.18}$$

As was mentioned before, the second assumption on the random phase results in the necessity of carrying out the field analysis by means of the expected value $E(\,)$, the standard deviation $\varepsilon(\,)$ etc. Below, their final formulae for the intensity $I(\vartheta)$, the intensity directivity function $s^I(\vartheta)$ and the power output $\mathcal{P}$, calculated basing on the results obtained for multifrequency excitation [20] are presented.

The expected value and the variance [10] of the sound intensity are equal to, respectively

$$E(I(\vartheta)) = \frac{1}{2\varrho_0 c}\int\limits_{\omega\in B}\sum_{l=0}^{N(\omega)} P_l^2\, d\omega \tag{2.19}$$

and

$$\operatorname{var}(I(\vartheta)) = \frac{1}{2(\varrho_0 c)^2}\int\limits_{\omega\in B}\sum_{\substack{l,m\\ l<m}}^{N(\omega)} (P_l\, P_m)^2\, d\omega\,. \tag{2.20}$$

Theoretical results were compared with experimental data for the one third octave (tierce) white noise with the mid-frequencies $f_0 = 8\,\mathrm{kHz}$ and $f_0 = 10\,\mathrm{kHz}$.

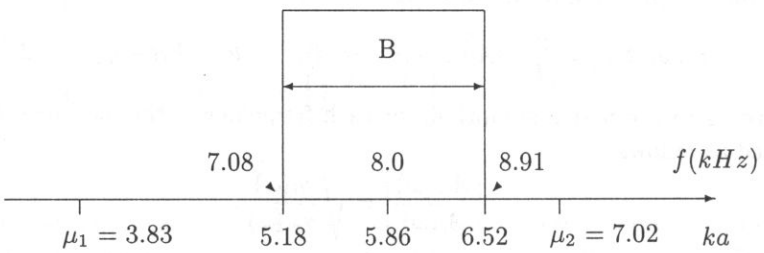

Fig. 2. Third-octave passband in the first experiment. Note constant density of energy distribution.

The first band, Fig. 2, covers the range of frequencies from 7.08 kHz to 8.91 kHz, which for considered duct 0.04 m in radius corresponds to the values of the dimensionless wavenumber ka from 5.18 to 6.52, so the number of modes remains constant, $N(\omega) = 2$, in the whole band. The second band, Fig. 3, lowest and uppest frequencies are equal to 8.91 kHz and 11.2 kHz, so the ka parameter changes within the range $[6.52 \div 8.22]$, crossing the third root, $\mu_2 = 7.02$, of he Bessel function J_1. Thus, the number of modes excited in the duct changes within the band being equal $N(\omega) = 2$ for $ka \leq \mu_2$ and $N(\omega) = 3$ for $ka > \mu_2$.

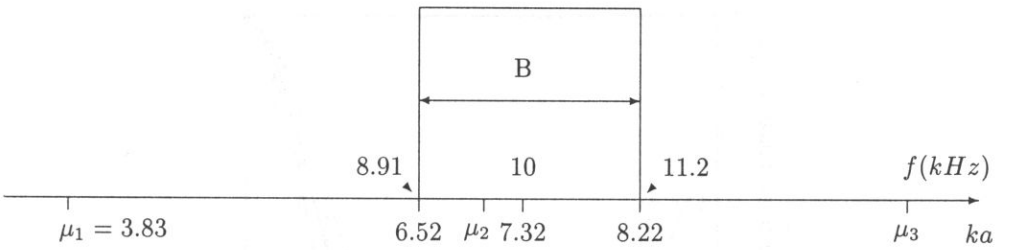

Fig. 3. Third-octave passband in the second experiment.

3. Physical quantities describing the far field

3.1. The intensity and the pressure directivity characteristics

The relative intensity directivity function was defined [20] as the intensity in a given direction referred to its expected value on the axis (the forward radiation) $s^I(\vartheta) = I(\vartheta)/E(I(\pi))$.

The next two formulae present its expected value and the standard deviation [10, 21]

$$E(s^I(\vartheta)) = \frac{E(I(\vartheta))}{E(I(\pi))} = \frac{\int\limits_{\omega\in B} \sum\limits_{l=0}^{N(\omega)} P_l^2(\omega,\vartheta)\, d\omega}{\int\limits_{\omega\in B} \sum\limits_{l=0}^{N(\omega)} P_l^2(\omega,\pi)\, d\omega}, \tag{3.1}$$

$$\varepsilon(s^I(\vartheta)) = \frac{\sqrt{\mathrm{var}(I(\vartheta))}}{E(I(\vartheta))} = \frac{\sqrt{2\int\limits_{\omega\in B} \sum\limits_{\substack{l,m \\ l<m}}^{N(\omega)} (P_l\, P_m)^2\, d\omega}}{\int\limits_{\omega\in B} \sum\limits_{l=0}^{N(\omega)} P_l^2\, d\omega}. \tag{3.2}$$

Defining the pressure directivity function as the pressure in a given direction referred to its expected value on the axis (the forward radiation) $s^p(\vartheta) = p_{rms}(\vartheta)/E(p_{rms}(\pi))$, and basing on considerations enclosed in [21] we obtain

$$E(s^p(\vartheta)) \cong \sqrt{E(s^I(\vartheta))}, \tag{3.3}$$

$$\varepsilon(s^p(\vartheta)) \cong \frac{1}{2}\varepsilon(s^I(\vartheta)). \tag{3.4}$$

Theoretical results, calculated with the help of the presented model assuming additionally equipartition of energy between the modes composing the incident wave, and their phases constituting, for each frequency, a set of mutually independent random variables, compared with experimental data are presented on graphs.

Analysing Figs. 4–7 one sees that the accordance between theory and experiment is quite good for the forward radiation, when rays bent from the axis of no more than 30 deg

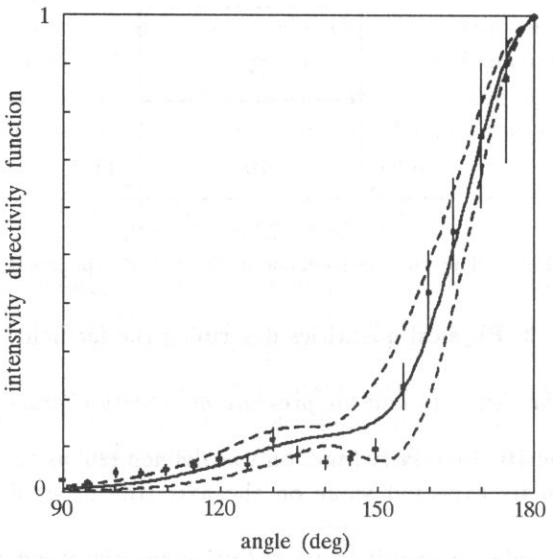

Fig. 4. Relative intensity directivity function $s^I(\vartheta)$ for the third-octave white noise band excitation with nominal centre frequency $f_0 = 8\,\text{kHz}$). The expected value $E(s^I(\vartheta))$ (continuous line), values of $E(s^I(\vartheta))(1 \pm \varepsilon)$, (dashed lines) ε being the standard deviation. Stars indicate the experimental data and bars the measurement errors.

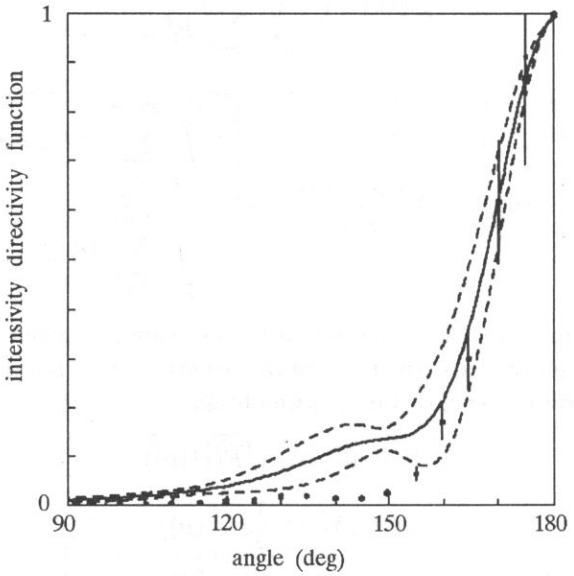

Fig. 5. Same as Fig. 4, but for centre frequency $f_0 = 10\,\text{kHz}$.

are considered (range 150 – 180 deg on drawings, note that angle 180 deg corresponds to the forward radiation) and deteriorates for smaller angles. The last effect is especially visible on Figs. 5 and 7, that is for the band with the centre frequency equal to 10 kHz,

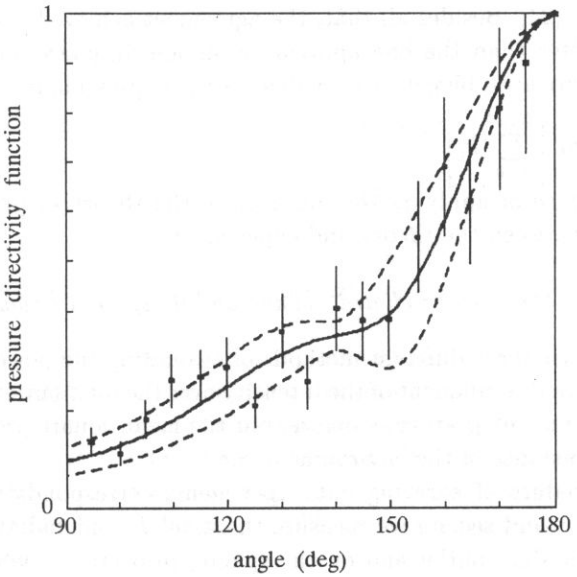

Fig. 6. Relative pressure directivity function $s^p(\vartheta)$ for the third-octave white noise band excitation with nominal centre frequency $f_0 = 10\,\text{kHz}$. The expected value $E(s^p(\vartheta))$ (continuous line), values of $E(s^p(\vartheta))(1 \pm \varepsilon)$, (dashed lines) ε being the standard deviation. Stars indicate the experimental data and bars the measurement errors.

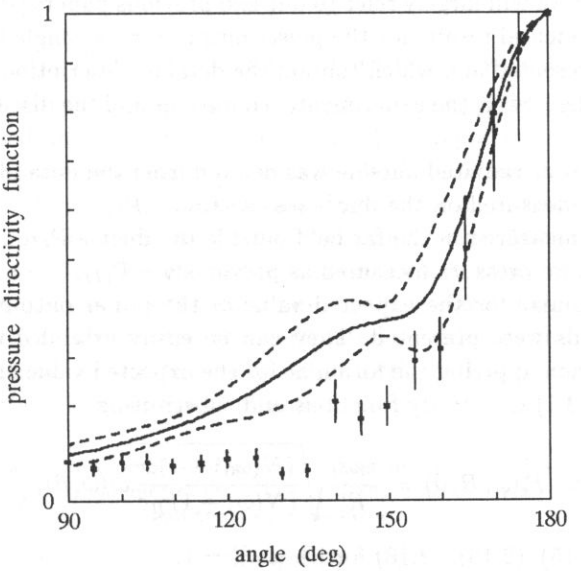

Fig. 7. Same as Fig. 6, but for centre frequency $f_0 = 10\,\text{kHz}$.

theoretical predictions exceeding experimental data. It may stem from the tendency of the physical system to occupy the state of the lowest possible energy and the fact, that the directivity characteristic representing the most probable state lies below the line of

the expected value [24]. Besides all that, the agreement achieved assuming the random phase is much better than the one applying all-modes-in-phase model, for which the theoretical values are even bigger. It is evident as the expression in bracket in Eq. (2.17) takes then the form $\left[\sum_{l=0}^{N(\omega)} P_l\right]^2$.

The inconvenience of applying the methods of the theory of probability results in better agreement between the theory and experiment.

3.2. The power radiated outside and its space distribution

There are at least three different methods of evaluating the power radiated outside: integrating the normal component of the intensity over the duct outlet or over a sphere in the far field outside or integrating as before, but the mean square pressure p_{rms}^2 divided by the specific impedance of the environment $\varrho_0 c$.

A certain procedure of carrying out experiments corresponds to each theoretical method. In the first and second we measure the axial I_z and radial I_R components of the intensity on the duct outlet and on the sphere, respectively, while in the third we measure the mean pressure p_{rms} on the sphere in the far field.

Because of assumed random phases we should compare the experimental data with the expected value of the power output and the measurement error with the standard deviation.

In the following we will largely refer to our two previous papers [19, 20] in which theoretical and experimental results for the power output for the single tone and multitone excitations were presented and which contain the detailed description of the three methods of evaluating the power, the experimental conditions and the discussion of measuring errors.

In short, the power radiated outside was derived from the data of
- the intensity measured on the duct cross-section – $\mathcal{P}_I$,
- the intensity measured in the far field outside the duct – $\mathcal{P}_{II}$,
- the mean square pressure measured as previously – $\mathcal{P}_{III}$.

In [20] the formulae for the expected value of the power output corresponding to these three methods were presented. They can be easily extended on the case of the white noise excitation applying the formulae for the expected value of the pressure (3.3) and the intensity (3.1) directivity functions and substituting

$$P_l(\omega, R, \vartheta) = \frac{\varrho_0 \omega_0}{R} \sqrt{\frac{(N(\omega_0)+1)\omega}{(N(\omega)+1)\gamma_l c}}\, d_l(\omega, \vartheta), \tag{3.5}$$

calculated from (2.15)–(2.16), (2.18) for $|A_0(\omega_0)| = 1$.

Focusing on methods applying the far–field relations, which are of our main interest, two formulae for deriving the power output will be reminded

$$E(\mathcal{P}_{II}) = 2\pi R^2 E(I(\pi)) \int_0^{\pi} E(s^{(I)}(\vartheta)) \sin\vartheta \, d\vartheta\,, \tag{3.6}$$

$$E(\mathcal{P}_{III}) = \frac{2\pi R^2}{\varrho_0 c} E(p^2_{rms}(\pi)) \int_0^{\pi} E(s^{(p)}(\vartheta))^2 \sin\vartheta \, d\vartheta \,. \tag{3.7}$$

The standard deviation is calculated according to formula $\varepsilon(\mathcal{P}) = \sqrt{\mathrm{var}\mathcal{P}}/E(\mathcal{P})$, where

$$\mathrm{var}(\mathcal{P}) = E(\mathcal{P}^2) - E^2(\mathcal{P}) = 2\left(\frac{\pi R^2}{\varrho_0 c}\right)^2 \int_{\omega\in B} \sum_{\substack{l,m \\ l<m}}^{N(\omega)} \left(\int_0^{\pi} P_l \, P_m \sin\vartheta \, d\vartheta \right)^2 , \tag{3.8}$$

exchanging in the expression for the variance [20] summation for integration over frequencies.

Another difficulty which arises when comparing theory with experiment comes from the fact that the assumptions of the model allow only for determining the relative amplitudes of modes and thus we have to incorporate one experimental data into the theoretical formulae to derive the so-called scale factor. In the presented analysis a point on the axis ($\vartheta = 180°$) served as a scaling point, so we substituted theoretical value $E(I(\pi))$ by $\widetilde{I}(\pi)$ and $E(p^2_{rms}(\pi))$ by $\widetilde{p}^2_{rms}(\pi)$. Tilde over a symbol means, in this paper, the experimental value.

Discussion of errors carried in [19, 20], which results are valid also in the considered case, led to expressions for the measuring error and the method uncertainty (the last stemmed from the assumption on random phase) and allowed for deriving a criterion of correctness of the proposed model [19]

$$\Delta L_{\mathcal{P}} \leq L_{\delta} \,, \tag{3.9}$$

where $\Delta L_{\mathcal{P}} = \left| 10 \log E(\mathcal{P}')/\widetilde{\mathcal{P}} \right|$ is the method uncertainty, while the total error of the experiment, in decibels, is equal to $L_{\delta} = -10\log(1 - \delta - \delta_{\Delta S}/1 + \varepsilon_{\mathcal{P}} + \delta)$, where $E(\mathcal{P}')$ denotes the expected value of the power obtained by replacing the theoretical value $E(I(\pi))$ by the adequate experimental data $\widetilde{I}(\pi)$, $\widetilde{\mathcal{P}}$ denotes measured power, δ – error in the intensity or the mean square pressure data, while $\delta_{\Delta S}$ denotes error in surface estimation when approximating the integral by a finite sum. The relative error in the pressure and the intensity measuring data is assumed to be the same in all measuring data, not exceeding 0.2, same as the maximum of the surface error.

The experimental results for the power radiated outside, for the third-octave white noiseband with nominal centre frequency $f_0 = 8\,\mathrm{kHz}$ and $f_0 = 10\,\mathrm{kHz}$, obtained by means of three methods are depicted in Table 1.

Table 1. Values of the sound power level $L_{\mathcal{P}}$ measured by means of the three methods, estimated from the theory $L_{E(\mathcal{P}')}$, the uncertainty $\Delta L_{\mathcal{P}'}$ resulting from the applied theoretical model and the measuring error L_{δ}.

nominal centre frequency	experimental			theoretical		uncertainty		error
f_0 (kHz)	$L_{\mathcal{P}_I}$ (dB)	$L_{\mathcal{P}_{II}}$ (dB)	$L_{\mathcal{P}_{III}}$ (dB)	$L_{E(\mathcal{P}'_{II})}$ (dB)	$L_{E(\mathcal{P}'_{III})}$ (dB)	$\Delta L_{\mathcal{P}_{II}}$ (dB)	$\Delta L_{\mathcal{P}_{III}}$ (dB)	$L_{\delta_{II,III}}$ (dB)
8.0	78.9	80.0	77.6	80.1	77.2	0.1	0.4	4.1
10.0	81.0	80.1	76.7	83.5	80.2	3.4	3.5	4.0

The Table includes only the method uncertainty $\Delta L_{\mathcal{P}}$ and the measuring error L_δ for measurements taken in the far field because the upper frequencies became too big for the used microphone probe (the two 1/2 inches microphone sound intensity probe type face to face with the 6 mm spacer in between) what affected the experimental error.

From the results presented in the above table we conclude that the relation $\Delta L_{\mathcal{P}} \leq L_\delta$ is fulfilled for both tierces and for all measuring methods. As the experimental data fulfil the criterion of correctness we can say that at least they do not contradict the assumptions. Similar results were obtained for the single tone [19] and the multitone [20] excitation.

Many applications demand the knowledge of the space distributions of the energy radiated from the duct outlet, which is described by the power-gain function, $\mathcal{G}(\vartheta, \phi)$, referring the amount of energy radiated into a certain solid angle to the total energy radiated outside.

For axisymmetrical excitation, according to the definition, we obtain

$$\mathcal{G}(\vartheta) = 4\pi R^2 \frac{I(\vartheta)}{\mathcal{P}(\text{rad})}. \tag{3.10}$$

Experimental results versus the angle ϑ are presented in Table 2, pointing at a strong radiation in the vicinity of the axis.

Table 2. Experimental results for the power-gain function versus angle ϑ on a front hemisphere, as data for backward radiation were negligible small.

angle deg	nominal centre frequency $f_0 = 8$ kHz	nominal centre frequency $f_0 = 10$ kHz
ϑ	$\mathcal{G}$	$\mathcal{G}$
90	0.50	0.26
95	0.43	0.15
100	0.81	0.18
105	0.81	0.17
110	0.96	0.17
115	1.08	0.24
120	1.38	0.38
125	1.17	0.49
130	2.15	0.96
135	1.54	1.01
140	1.23	0.80
145	1.43	0.81
150	1.78	1.34
155	4.23	3.36
160	7.84	8.67
165	10.22	15.06
170	13.95	30.86
175	16.19	43.41
180	18.59	49.84

The integrand of $\mathcal{G}(\vartheta, \phi)$ over the entire solid angle is equal to 4π, so the integrand of (3.7) over the angle ϑ is equal to 2. The results obtained from the experimental data, when replacing integration by summation, are presented in Table 3 and show very good agreement with the theory. If the experimental data fulfil this condition we can say that they do not contradict the assumptions.

Table 3. Experimental results for the power-gain function, when the theory predicts the value equal to 2.

nominal centre frequency f_0 [kHz]	$\sum G_I(\vartheta) \sin\vartheta \, \Delta\vartheta$
8.0	1.983
10.0	1.953

4. Conclusions and possible applications

The paper presents a certain model for qualitative and also quantitative description of the narrow band sound field radiated from axially excited cylindrical duct in the absence of the mean flow. The last two assumptions were set because of some limitations of the experimental set-up to make comparison with the experiment possible. Nevertheless the results can be generalised by solving the wave equation with sources. The starting formulae were derived for the semi-infinite duct and take into account diffraction phenomena at the open end. Thus they are valid for the duct long in comparison to the wave length and with only one outlet – provided at the other end with sound absorbing material. These features are found in many duct-like devices, to mention only heating and ventilation systems, cars and planes exhausts, factory chimneys etc., what makes investigation on the problem interesting from both, theoretical and practical, points of view. In the light of the above we expect many potential applications in problems requiring the knowledge of the directivity characteristics or the power output.

The experimental results presented in the paper show that good agreement between the theory and experiment has been obtained, what in a way verifies the model we proposed. Considering the directivity characteristics, the random phase assumption approaches theoretical predictions to measurement data much better than commonly used all-modes-in-phase assumption.

Especially good agreement was obtained for the power output, which we found very promising in applying the circular duct as a reference source. As was shown in Table 1 the power estimated by means of the model and single measurement on the axis in the far field differs from the one calculated following one of the well known procedures described above less than the experimental error. There from origins the idea to estimate the power output basing at only one measurement on the axis.

The paper is considered to be a step forward in deriving a procedure of evaluating, or at least estimating, the power radiated outside measuring the pressure or the intensity in only one point. It needs preparation of a set of numerical programs computing the expected value and the standard deviation along the formulae (3.6), (3.8), (2.15), but we hope to present it in the next paper.

References

[1] U. BOLLETER, M.J. CROCKER, *Theory and measurement of modal spectra in hard-walled cylindrical duct*, J. Acoust. Soc. Am., **51**, 1439–1447 (1972).

[2] P.E. DOAK, *Excitation, transmission and radiation of sound from source distributions in hard-walled ducts of finite length. I. The effects of duct cross-section geometry and source distribution space-time pattern*, J. Sound Vib., **31**, 1, 1–72 (1973).

[3] P.E. DOAK, *Excitation, transmission and radiation of sound from source distributions in hard-walled ducts of finite length. II. The effects of duct length*, J. Sound Vib., **31**, 2, 137–174 (1973).

[4] DUHAMEL, *Improvement of noise barrier efficiency by active control*, Acta Acustica, **3**, 1, 25–35 (1995).

[5] S.J. ELLIOT, P. JOSEPH, P.A. NELSON, M.E. JOHNSON, *Power output minimization and power absorption in the active control of sound*, J. Acoust. Soc. Am., **90**, 5, 2501–2512 (1991).

[6] G.F. HOMICZ, J.A. LORDI, *A note on the radiative directivity patterns of duct acoustic modes*, J. Sound and Vib., **41**, 283–290 (1975).

[7] M.E. JOHNSON, S.J. ELLIOT, *Measurement of acoustic power output in the active control of sound*, J. Acoust. Soc. Am., **93**, 1453–1459 (1993).

[8] G.W. JOHNSTON, K. OGIMOTO, *Sound radiation from a finite length unflanged circular duct with uniform axial flow. I. Theoretical analysis*, J. Acoust. Soc. Am., **68**, 1858–1870 (1980).

[9] G.W. JOHNSTON, K. OGIMOTO, *Sound radiation from a finite length unflanged circular duct with uniform axial flow. II. Computed radiation characteristics*, J. Acoust. Soc. Am., **68**, 1871–1883 (1980).

[10] W. LEDERMANN, *Handbook of applicable mathematics*, Wiley & Sons, N. York 1980.

[11] H. LEVINE, J. SCHWINGER, *On the radiation of sound from an unflanged circular pipe*, Phys. Rev., **73**, 383–406 (1948).

[12] B. NOBLE, *Methods based on the Wiener–Hopf technique for the solution of partial differential equations*, Pergamon Press, London – New York 1958.

[13] A.D. RAWLINS, *Radiation of sound from an unflanged rigid cylindrical duct with an acoustically absorbing internal surface*, Proc. R. Soc. London, **A 361**, 65–91 (1978).

[14] E.J. RICE, *Multi-modal far-field acoustic radiation pattern using mode cut-off ratio*, AIAA Journal, **16**, 906–911 (1978).

[15] E. SKUDRZYK, *The foundations of acoustics*, Springer-Verlag, Wien–New York 1971.

[16] M.A. SWINBANKS, *The active control of sound propagation in long ducts*, J. Sound Vib., **27**, 3, 411–436 (1973).

[17] A. SNAKOWSKA, *The acoustic far field of an arbitrary Bessel mode radiating from a semi-infinite unflanged cylindrical wave-guide*, Acustica, **77**, 53–62 (1992).

[18] A. SNAKOWSKA, *Directivity patterns of the acoustic field radiated from a semi-infinite unflanged hard walled circular duct*, Journal de Physique III, 2, C1-653–656 (1992).

[19] A. SNAKOWSKA, H. IDCZAK, *The acoustic power radiated from the outlet of a hard-walled circular duct – theory and measurement*, Acta Acustica, **3**, 119–128 (1995).

[20] A. SNAKOWSKA, H. IDCZAK, *Prediction of multitone sound radiation from a circular duct*, Acustica-Acta Acustica, **83**, 955–962 (1997).

[21] A. SNAKOWSKA, H. IDCZAK, B. BOGUSZ, *Modal anlysis of the acoustic field radiated from an unflanged cylindrical duct – theory and measurement*, Acustica-Acta Acustica, **82**, 2, (1996).

[22] A. SNAKOWSKA, R. WYRZYKOWSKI, *Calculation of the acoustical field of a semi-infinite cylindrical wave-guide by means of the Green function expressed in cylindrical coordinates*, Archives of Acoustics, **11**, 261–285 (1986).

[23] A. SNAKOWSKA, R. WYRZYKOWSKI, *Impedance of the semi-infinite unbaffled cylindrical waves quide outlet*, Archives of Acoustics, **13**, 1-2 (1988).

[24] J.K. SNAKOWSKI, *Private communication.*

[25] L.A. VAJNSHTEJN, *The theory of sound waves in open tubes*, Res. Rep. No. EM– 63, Inst. Math. Sci., N. Y. U., 87–116 (1954).

[26] L.A. WEINSTEIN, *The theory of diffraction and the factorization method (Generalised Wiener-Hopf technique)*, Golem Press, Boulder, Colorado 1969.

[27] A.C. ZANDER, C.H. HANSEN, *Active control of higher-order acoustic modes in ducts*, J. Acoust. Soc. Am., **92**, 244–257 (1992).